Authors' Responses to the Reviewers' Comments

First and foremost, we would like to sincerely thank the reviewers and the editor for their valuable comments, constructive suggestions, and critical assessments, which have greatly contributed to improving our manuscript.
Below, we provide detailed point-by-point responses to all comments and questions raised. As the manuscript has undergone substantial revision, and several reviewers raised overlapping concerns, it would not be practical to use different colours in the tracked-changes manuscript to indicate which modifications were made in response to specific reviewers' comments. Therefore, to facilitate the review process, we have reproduced relevant excerpts from the revised manuscript within our detailed responses, highlighting these passages in blue.
All revisions and modifications are clearly indicated in the tracked-changes version of the manuscript.

Response to Reviewer 1

We sincerely thank Reviewer 1 for the positive assessment and the detailed and constructive comments. Following these suggestions, we revised the Introduction, Methods, Results and Discussion, and added a vertically resolved MERRA-2 dust analysis to better assess the presence of Saharan dust at cirrus-relevant altitudes.

Comment: The abstract should be as compact as possible
Response: Thank you. The Abstract has been shortened and reorganized to focus on the motivation, methods, and principal findings:

Saharan mineral dust is an important source of ice-nucleating particles, yet the long-term evolution of its relationship with upper-tropospheric ice clouds remains poorly constrained. Here, we investigate dust–cloud interactions over Hungary during 2001–2025 using MERRA-2, MODIS, and HIRS data, focusing on 276 independently identified Saharan dust events (SDEs). Vertically resolved MERRA-2 dust fields were used to quantify mineral dust at 7–12 km, allowing cloud properties to be compared between SDEs with different upper-tropospheric dust abundances and low-dust reference conditions. SDEs with high Dust7–12 were characterized by enhanced cirrus reflectance and high-cloud fraction and by higher, colder cloud tops in all seasons. The response was particularly coherent in spring, when cirrus reflectance and high-cloud fraction were 272% and 133% higher, respectively, effective ice particle radius was 7.2% smaller, and outgoing longwave radiation was 14.4% lower than under low-dust conditions. Springtime five-year composites showed no monotonic increase in Dust7–12, whereas the cirrus-reflectance enhancement increased from 143% in 2001–2005 to 398% in 2021–2025. These results indicate an increasingly pronounced springtime cirrus optical response during SDEs containing substantial dust at cirrus-relevant altitudes, while other cloud properties exhibit more variable long-term behaviour.

Comment: A more appropriate introduction into the cirrus literature would be desirable.
Response: We agree. The Introduction has been expanded to provide a broader background on cirrus formation, radiative effects, homogeneous and heterogeneous ice nucleation, and mineral-dust INPs. The recommended studies have been incorporated:

Their radiative effect depends strongly on cloud altitude, optical thickness, ice crystal concentration, particle size and habit, and may therefore range from shortwave cooling to pronounced longwave warming (Heymsfield et al., 2017; Liou, 1986). Cirrus clouds also encompass a wide variety of formation pathways and microphysical states, ranging from in situ cirrus formed directly at low upper-tropospheric temperatures to liquid-origin cirrus developing from the glaciation of pre-existing mixed-phase clouds (Krämer, 2016, 2020; Krämer et al., 2025). Their formation is critically controlled by temperature, ice supersaturation, vertical motion, and the availability and ice-nucleating ability of aerosol particles. Consequently, relatively small changes in the thermodynamic environment or aerosol population may alter ice crystal number concentrations and cloud optical properties, with potential consequences for cirrus persistence and radiative effects (Kanji et al., 2017; Knopf and Alpert, 2023).
A central challenge in representing cirrus clouds in atmospheric models is the competition between homogeneous freezing and heterogeneous ice nucleation. Homogeneous freezing of solution droplets generally requires high ice supersaturation and can produce large numbers of ice crystals, whereas heterogeneous nucleation on ice-nucleating particles can initiate ice formation at lower supersaturation and modify the subsequent evolution of the cloud (Kärcher et al., 2022, 2023).
(…)
Mineral dust is particularly relevant in this context because it represents one of the most important atmospheric sources of ice-nucleating particles, although its activity depends strongly on particle concentration, mineralogical composition, temperature, and nucleation mode (DeMott et al., 2003, 2010; Niemand et al., 2012; Ullrich, 2017). Model simulations therefore indicate that the response of cirrus clouds to mineral dust is not necessarily monotonic: enhanced heterogeneous nucleation may modify or suppress subsequent homogeneous freezing, while variations in vertical velocity and supersaturation can substantially change the resulting ice crystal population (Kärcher et al., 2022, 2023). Assessing dust–cirrus interactions thus requires consideration not only of atmospheric dust loading, but also of whether mineral dust reaches cirrus-forming altitudes and encounters thermodynamic and dynamical conditions favourable for heterogeneous ice nucleation.
In this context, Saharan mineral dust plays a particularly important role (Ansmann et al., 2019; Seifert et al., 2023; Weger et al., 2018). During long-range transport events, large quantities of mineral dust can reach Europe, including Central Europe (Ansmann et al., 2003; Pey et al., 2013; Rogora et al., 2004; Salvador et al., 2022; Varga, 2020). Mineral aerosol particles, especially those rich in K-feldspar, quartz and calcite, are known to act as highly efficient heterogeneous ice nuclei under the low-temperature conditions of the upper troposphere (Atkinson et al., 2013; Chatziparaschos et al., 2023; Harrison et al., 2019; Hoose et al., 2008; Hoose and Möhler, 2012; Seifert et al., 2010). The presence of mineral dust can promote heterogeneous ice nucleation at lower ice supersaturation than required for homogeneous freezing and may thereby modify ice crystal populations and the optical and radiative properties of cirrus clouds (Kok et al., 2023; Storelvmo, 2017).

Comment: Lines 46–51: References on ice nucleation, Saharan dust observations, and feldspar.
Response: The recommended references have been incorporated, including Ansmann et al. (2003) on Saharan dust transport and Atkinson et al. (2013) on the ice-nucleating efficiency of feldspar.

In this context, Saharan mineral dust plays a particularly important role (Ansmann et al., 2019; Seifert et al., 2023; Weger et al., 2018). During long-range transport events, large quantities of mineral dust can reach Europe, including Central Europe (Ansmann et al., 2003; Pey et al., 2013; Rogora et al., 2004; Salvador et al., 2022; Varga, 2020). Mineral aerosol particles, especially those rich in K-feldspar, quartz and calcite, are known to act as highly efficient heterogeneous ice nuclei under the low-temperature conditions of the upper troposphere (Atkinson et al., 2013; Chatziparaschos et al., 2023; Harrison et al., 2019; Hoose et al., 2008; Hoose and Möhler, 2012; Seifert et al., 2010).

Comment: Are you sure that the basin-like topography favors accumulation of air masses after long-range transport and provides favorable conditions for the formation and persistence of high level clouds? Are there articles that confirm or support your hypothesis?
Response: We agree that this interpretation was too speculative. The text has been revised to avoid attributing upper-level cloud formation or persistence directly to the basin topography.

Comment: The study is based on hourly dust COLUMN mass density fields. In the case of a dust event, how sure can you be that that dust occurred at cirrus formation height level? Height information.
Response: We addressed this issue with a new vertically resolved MERRA-2 analysis. Dust exceeding 10^{-9} kg kg^{-1} was present at 7–12 km in 95.7% of the 276 SDEs, demonstrating frequent vertical overlap between Saharan dust and cirrus-relevant altitudes. This analysis has been added to the Methods and Results. The results of the vertical analyses were also plotted on a new figure.

Methods:
The threshold-based analysis extends this approach by progressively selecting days exceeding different column-dust levels, thereby characterizing dust-load-dependent cloud responses and their evolution across consecutive five-year periods without relying on a single arbitrary dusty-day threshold. Finally, vertically resolved MERRA-2 dust mass mixing ratios at 7–12 km were used to determine whether mineral dust was actually present at cirrus-relevant altitudes and whether cloud properties were more closely associated with upper-tropospheric dust than with total-column loading. Thus, these metrics address complementary aspects of the problem—event occurrence, total dust burden, dust-load dependence, and vertical dust–cloud co-occurrence—rather than representing alternative definitions of the same quantity.
(…)
To assess whether Saharan dust was present at altitudes relevant to cirrus formation, the total-column analysis was complemented with three-dimensional MERRA-2 aerosol fields. For each of the identified SDEs, 3-hourly dust mass mixing ratios for the five MERRA-2 dust size

bins (DU001–DU005) were extracted over the study domain from the native model-level aerosol product. Total dust mass mixing ratio (kg kg^{-1}) was calculated as the sum of the five size bins. Aerosol fields were matched to the corresponding three-dimensional MERRA-2 atmospheric fields, and the geometric height assigned to each model level was used to determine the actual altitude of the dust at every time step and grid point. This allowed the dust distribution to be evaluated independently of fixed model-level or pressure-level assumptions. Upper-tropospheric dust was primarily characterized over the 7–12 km altitude range, with additional calculations for the 7–8, 8–9, 9–10, and 10–12 km layers to examine the vertical dependence of the dust–cirrus relationship. Event-level mean dust mass mixing ratios were calculated from all grid points and 3-hourly time steps falling within each altitude interval. These vertically resolved dust metrics were subsequently compared with the MODIS and HIRS cloud properties used in the original analysis to determine whether cirrus responses were more closely associated with dust present at cirrus-relevant altitudes than with total-column dust loading.

(…)

To examine whether the vertical penetration of dust into the upper troposphere was associated with the magnitude of the cloud response, SDEs were additionally divided within each season according to their Dust7–12 values. Events below or equal to the seasonal median Dust7–12 concentration were classified as lower-upper-tropospheric-dust SDEs, whereas events above the seasonal median were classified as higher-upper-tropospheric-dust SDEs. The use of season-specific thresholds avoided applying a single concentration criterion to seasons characterized by substantially different upper-tropospheric dust distributions. Three complementary contrasts were then evaluated: (i) all SDE days versus low-dust reference days, (ii) lower- and higher-Dust7–12 SDE subsets separately versus the corresponding seasonal reference, and (iii) higher- versus lower-Dust7–12 SDEs directly. The latter comparison was used to determine whether cloud properties differed systematically among SDEs depending on the amount of mineral dust present at 7–12 km.

Results

3.2.2. Upper-tropospheric dust occurrence and comparison with column dust loading

The vertically resolved MERRA-2 analysis showed that mineral dust was frequently present at cirrus-relevant altitudes during the identified SDEs. Across the 276 events, the median event-mean dust mass mixing ratio in the 7–12 km layer was 9.63×10^{-8} kg kg^{-1} (Figure 3). Upper-tropospheric dust was not restricted to the lower part of this altitude range: the corresponding median was 8.33×10^{-9} kg kg^{-1} at 8–12 km and 4.37×10^{-9} kg kg^{-1} at 10–12 km. Of all SDEs, 264 (95.7%) exhibited event-mean dust mass mixing ratios exceeding 10^{-9} kg kg^{-1} between 7 and 12 km, while 204 (73.9%) exceeded 5×10^{-9} kg kg^{-1}, and 134 (48.6%) exceeded 10^{-8} kg kg^{-1}. Even when the analysis was restricted to 8–12 km, these thresholds were exceeded in 93.1%, 67.0%, and 44.6% of the events, respectively. At 10–12 km, 81.2% of the SDEs still exceeded 10^{-9} kg kg^{-1}.

The amount of dust at 7–12 km was also substantial relative to that at 3–7 km; the upper-tropospheric mean reached at least 30% of the 3–7 km value in 62% of the events and at least 50% in 35.5% of the events. These results demonstrate that, within MERRA-2, Saharan dust during the investigated events was generally not confined to the lower and middle

troposphere but frequently extended into the altitude range occupied by upper-level ice clouds.

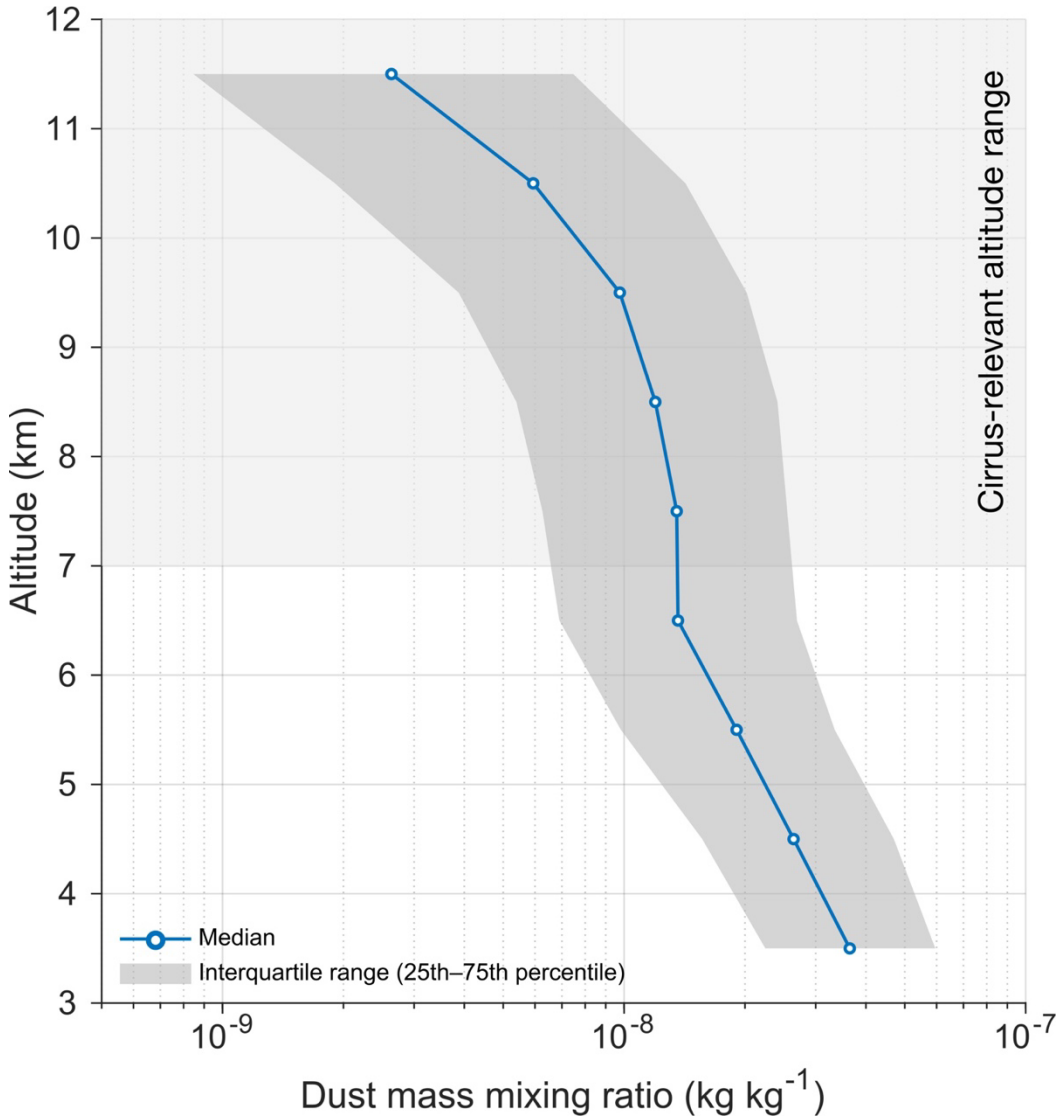

Figure 3. Vertical distribution of Saharan dust during the 276 identified SDEs. (The line shows the median MERRA-2 dust mass mixing ratio, with the shaded envelope representing the interquartile range, while the shaded 7–12 km layer indicates cirrus-relevant altitudes.)

Comment: How reliable are the small changes in MODIS effective ice-particle radius?
Response: We agree that relatively small changes in MODIS-derived effective ice-particle radius should be interpreted with caution, particularly because satellite retrievals are subject to uncertainties associated with cloud optical thickness, cloud heterogeneity, particle shape assumptions, and retrieval conditions.

In the revised manuscript, we have therefore placed greater emphasis on the statistical robustness and seasonal consistency of the observed differences rather than interpreting small changes in effective radius as direct evidence of dust-induced ice nucleation.
Our revised event-based analysis indicates that statistically significant differences in effective ice-particle radius are primarily confined to spring. During springtime Saharan dust events

characterized by high upper-tropospheric dust concentrations (Dust7–12), the median effective radius was 28.44 µm, compared with 30.65 µm under low-dust reference conditions, corresponding to a reduction of approximately 2.22 µm (7.2%; FDR-adjusted q ≈ 0.0012). Importantly, a separate comparison restricted entirely to independently identified Saharan dust events also revealed a significant difference between high- and low-Dust7–12 conditions (28.44 versus 31.90 µm, respectively; q ≈ 0.0023).
These two independent group comparisons provide statistical support for a springtime association between enhanced upper-tropospheric dust abundance and smaller retrieved ice-particle radii. However, statistical significance does not eliminate the systematic uncertainties inherent in satellite retrievals, and the observed differences should not be interpreted as precise measurements of dust-induced changes in ice-crystal size.

Spring exhibited a similarly coherent response, but additionally showed a significant reduction in effective ice particle radius. In high-Dust7–12 spring SDEs, the median effective radius was approximately 7% smaller than under low-dust reference conditions and was also significantly smaller than during lower-Dust7–12 SDEs. The simultaneous occurrence of enhanced cirrus reflectance, increased high-cloud fraction, and reduced effective ice particle size is compatible with a microphysical response involving enhanced ice nucleation. Mineral dust is an efficient ice-nucleating aerosol, and an increased number of ice crystals could contribute to greater cloud reflectance while reducing characteristic particle size. However, the absence of a similarly robust radius response in the other seasons indicates that this mechanism cannot be inferred universally from the present observations.

Comment: A reference to the model GAM would be fine.
Response: The statistical methodology has been completed with other analytical approaches and appropriate methodological description have been added. The revised analysis is performed on daily observations rather than cumulative threshold averages:

2.4. Event-based statistical analysis

To investigate whether the cloud properties associated with Saharan dust events depend on the presence of mineral dust at cirrus-relevant altitudes, an event-based analysis was performed using the 276 independently identified SDE days. Rather than relying primarily on correlations between dust concentration and individual cloud parameters, the analysis was designed to compare cloud states associated with SDEs against low-dust background conditions. Low-dust reference days were defined as non-SDE days for which the total-column dust mass remained below the 75th percentile (upper quartile) of the complete 2001–2025 daily dust distribution. This criterion yielded 6836 reference days and excluded the upper quartile of the total-column dust distribution, where substantial dust influence was more likely. All comparisons were performed separately for winter, spring, summer, and autumn to account for the pronounced seasonal variability in both Saharan dust transport and cloud conditions.
To examine whether the vertical penetration of dust into the upper troposphere was associated with the magnitude of the cloud response, SDEs were additionally divided within each season according to their Dust7–12 values. Events below or equal to the seasonal median Dust7–12 concentration were classified as lower-upper-tropospheric-dust SDEs, whereas events above the seasonal median were classified as higher-upper-tropospheric-dust

SDEs. The use of season-specific thresholds avoided applying a single concentration criterion to seasons characterized by substantially different upper-tropospheric dust distributions. Three complementary contrasts were then evaluated: (i) all SDE days versus low-dust reference days, (ii) lower- and higher-Dust7–12 SDE subsets separately versus the corresponding seasonal reference, and (iii) higher- versus lower-Dust7–12 SDEs directly. The latter comparison was used to determine whether cloud properties differed systematically among SDEs depending on the amount of mineral dust present at 7–12 km.
The analysis included cirrus reflectance, effective ice particle radius, low-, mid-, and high-level cloud fraction, cloud-top pressure, cloud-top temperature, and OLR. Because several variables exhibited non-normal distributions and unequal group sizes, group differences were evaluated using two-sided Mann–Whitney U tests. The magnitude and direction of the differences were quantified using rank-biserial correlation (rrb) as a non-parametric effect-size measure, with positive values indicating higher values in the first group and negative values indicating lower values. To control for multiple comparisons, p-values were adjusted using the Benjamini–Hochberg false discovery rate (FDR) procedure, with FDR-adjusted ($q<0.05$) considered statistically significant. Group medians were used to characterize the magnitude of the observed differences.
Because vertically resolved Dust7–12 data were available only for the 276 SDE days, upper-tropospheric dust concentrations could not be directly compared between SDE and reference days. Accordingly, the low-dust reference group was defined independently using total-column dust mass, whereas Dust7–12 was used specifically to stratify the SDE population according to the degree of upper-tropospheric dust presence. This design therefore tests whether the cloud state associated with SDEs differs from low-dust background conditions and, more specifically, whether these anomalies become more pronounced when larger amounts of mineral dust are present at cirrus-relevant altitudes.

Comment: About the large tables
Response: We agree. The table has been simplified.

Comment: The relationship between synoptic transport patterns and dust at cirrus altitudes should be clarified.
Response: We now distinguish between the large-scale transport environment and the actual vertical location of dust. The latter is independently assessed using the new vertically resolved MERRA-2 analysis. The different synoptic types were discussed in detail in the cited papers by Varga et al..

Comment: You discuss effective-radius tendencies of 30.3, 29.9, and 28.2 micrometer…
Response: We agree that differences of only a few micrometres should not be overinterpreted. The revised manuscript therefore treats the effective-radius response as weak and does not use it as evidence for a major long-term microphysical change.

Comment: Line 251-255: You discuss Table 2, but you did not mention or introduce Table 2 in the main text body? Should be improved! Could be done in line 251.
Response: That table has been removed.

Comment: Are middle and high-level cloud fractions somewhere precisely defined? If yes, please indicate here where that was done, as a reminder. Please provide clear definitions somewhere.
Response: Definitions have been added to the Methods. MERRA-2 low-, middle-, and high-level cloud fractions correspond to the surface–700 hPa, 700–400 hPa, and above-400 hPa layers, respectively. The figure captions have also been clarified.

In MERRA-2, low-, middle-, and high-level cloud fractions correspond to clouds occurring between the surface and 700 hPa, 700 and 400 hPa, and above 400 hPa, respectively. These pressure ranges approximately correspond to altitudes of 0–3 km, 3–7 km, and >7 km, although their actual geometric heights vary with atmospheric conditions.

Comment: The interpretation should consider the competition between homogeneous and heterogeneous ice nucleation.
Response: We agree. The revised manuscript now explicitly discusses this competition based on Kärcher et al. (2022, 2023) and avoids assuming that increased mineral-dust INPs necessarily produce more ice crystals.

A central challenge in representing cirrus clouds in atmospheric models is the competition between homogeneous freezing and heterogeneous ice nucleation. Homogeneous freezing of solution droplets generally requires high ice supersaturation and can produce large numbers of ice crystals, whereas heterogeneous nucleation on ice-nucleating particles can initiate ice formation at lower supersaturation and modify the subsequent evolution of the cloud (Kärcher et al., 2022, 2023).
(…)
Homogeneous freezing of solution droplets generally requires high ice supersaturation and can produce large numbers of ice crystals, whereas heterogeneous nucleation on ice-nucleating particles can initiate ice formation at lower supersaturation and modify the subsequent evolution of the cloud (Kärcher et al., 2022, 2023). Mineral dust is particularly relevant in this context because it represents one of the most important atmospheric sources of ice-nucleating particles, although its activity depends strongly on particle concentration, mineralogical composition, temperature, and nucleation mode (DeMott et al., 2003, 2010; Niemand et al., 2012; Ullrich, 2017). Model simulations therefore indicate that the response of cirrus clouds to mineral dust is not necessarily monotonic: enhanced heterogeneous nucleation may modify or suppress subsequent homogeneous freezing, while variations in vertical velocity and supersaturation can substantially change the resulting ice crystal population (Kärcher et al., 2022, 2023). Assessing dust–cirrus interactions thus requires consideration not only of atmospheric dust loading, but also of whether mineral dust reaches cirrus-forming altitudes and encounters thermodynamic and dynamical conditions favourable for heterogeneous ice nucleation.

Comment: Figure 2 is the highlight of the paper! Again, I miss a clear definition of cloud cover and defined height regions for low, mid, and high clouds.
We need (a), (b), (c), etc.... within the six different panels.
Response: The definitions have been added, and table has been completed.

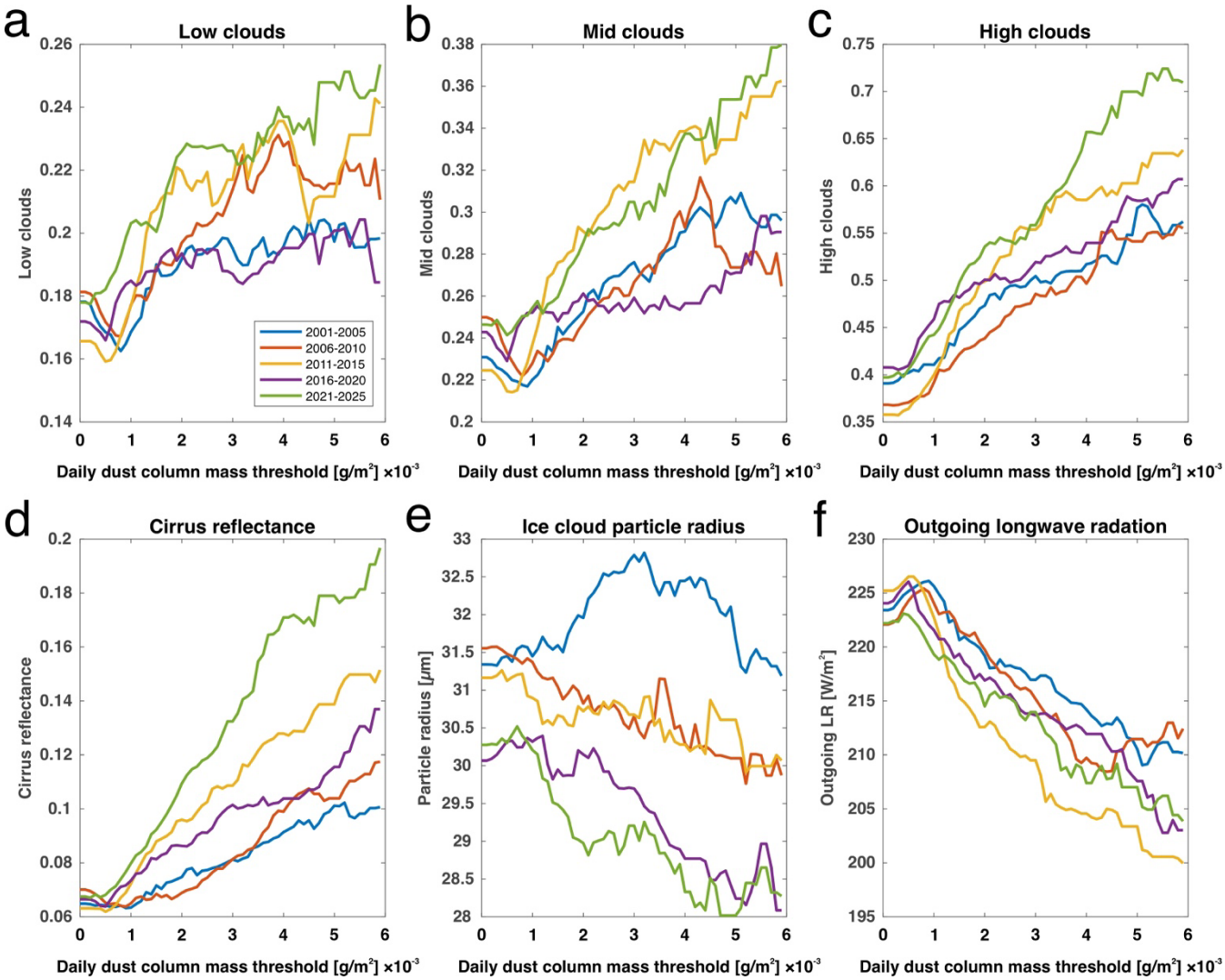

Figure 4. Variations in the investigated atmospheric and cloud-physical parameters as a function of daily dust column mass density thresholds during 2001–2025, presented for consecutive five-year periods. Panels show (a) low-, (b) middle-, and (c) high-level area-averaged cloud fractions, (d) cirrus reflectance, (e) ice-cloud effective particle radius, and (f) outgoing longwave radiation.

Comment: Can the direct dust effect on OLR be separated from the cirrus effect?
Response: No. We have clarified that our analysis cannot unambiguously separate these effects. OLR is therefore interpreted as an integrated radiative signature associated with dust-loading conditions rather than as an isolated cirrus radiative effect.

Across all five-year periods, progressively higher dust-loading thresholds were associated with lower OLR values. The magnitude and absolute level of this response varied among periods, with particularly low OLR values under high dust-loading conditions during 2011–2015 and 2016–2020. These results demonstrate a persistent dust-load dependence of springtime OLR, but do not indicate a uniform monotonic strengthening of the relationship over the full 25-year period.
It should be noted that the observed OLR response cannot be attributed exclusively to dust-associated changes in cirrus, because mineral dust itself contributes to the longwave

radiative balance. The OLR variations are therefore interpreted here as an integrated radiative signature associated with dust-loading conditions rather than as an isolated cirrus radiative effect.

Comment: Atmospheric dynamics should be included in the Discussion.
Response: We agree. The Discussion now considers vertical velocity, wind shear, turbulence, and ice supersaturation, following Pieper et al. (2026) and Juurikkala et al. (2026). We emphasize that the observed relationships may reflect combined aerosol, thermodynamic, and dynamical controls.

The pronounced seasonal differences further suggest that upper-tropospheric dust abundance alone is insufficient to determine the cloud response. In summer, enhanced Dust7–12 was most clearly associated with increased high-cloud fraction, whereas autumn exhibited particularly pronounced differences in cloud-top pressure and temperature. Such differences are consistent with the strong dependence of ice-cloud formation on the thermodynamic and dynamical environment. Temperature, ice supersaturation, vertical motion, and moisture availability may determine whether mineral dust reaching 7–12 km can effectively participate in ice formation and how the resulting cloud field develops. The seasonal dependence therefore provides an important indication that the observed dust–cloud relationship is conditional on the atmospheric environment.
The vertically resolved results also help explain why relationships based on total-column dust loading were comparatively weak. Total-column dust combines aerosol located at very different altitudes, much of which may have limited relevance to upper-tropospheric ice-cloud formation. Consequently, a strong SDE can exhibit high column-integrated dust loading while containing relatively little mineral dust near cirrus-forming levels. Explicit consideration of Dust7–12 reduces this vertical mismatch and reveals substantially clearer differences between events characterized by relatively low and high upper-tropospheric dust abundance. This emphasizes the importance of representing aerosol vertical distribution, rather than column loading alone, when investigating mineral dust–cirrus interactions.
Nevertheless, the observed differences should not be interpreted as direct evidence of dust-induced ice nucleation. Saharan dust reaching the upper troposphere is transported by atmospheric circulation that simultaneously determines vertical motion, humidity, temperature, and cloud formation. The high-Dust7–12 and low-Dust7–12 SDE subsets may therefore also represent different meteorological regimes. The present results demonstrate that upper-tropospheric dust occurrence is closely associated with distinct cloud states, but separating direct aerosol microphysical effects from the meteorological conditions responsible for both vertical dust transport and cloud development requires additional thermodynamic and dynamical information.
The complementary total-column threshold analysis also indicated increasing middle-level cloud fraction at higher dust-loading thresholds, suggesting that the observed relationships are not restricted to the classical cirrus altitude range. This suggests that the influence of Saharan dust may extend beyond classical cirrus formation and potentially affect cloud systems developing within the mixed-phase temperature regime. The temporal evolution of the dust–cloud relationship cannot be interpreted solely in terms of changes in mineral-dust INP availability. Cirrus nucleation and subsequent cloud development are also strongly controlled by the dynamical environment, including vertical velocity, wind shear, turbulence, and the associated variability in ice supersaturation. Recent observations of dusty cirrus and

large-eddy simulations indicate that changes in turbulence and updraft strength can substantially modify ice crystal nucleation, cloud structure, and persistence even under comparable aerosol conditions (Juurikkala et al., 2026; Pieper et al., 2026). Thus, the observed changes in cirrus properties during Saharan dust events may reflect a combined influence of mineral-dust availability and concurrent changes in upper-tropospheric dynamics rather than an aerosol effect alone.

Comment: Could the upper-tropospheric fraction of dust have increased over time?
Response: We examined this using vertically resolved MERRA-2 data. The 7–12 km dust mass mixing ratio showed no significant monotonic trend over 2001–2025, suggesting that the temporal changes cannot be explained simply by increasing upper-tropospheric dust abundance.

Comment: Are changes of only a few micrometres in effective radius physically meaningful?
Response: We agree that these differences are small. Their interpretation has therefore been substantially weakened, and the main conclusions are based on the more robust changes in cirrus reflectance, high-cloud fraction, and cloud-top properties.

Comment: The DIBS case should be attributed to the appropriate Ansmann et al. (2019) paper.
Response: Thank you. The citation has been corrected and the unnecessary Ansmann et al. (2019b) reference has been removed.

Direct observational evidence for this mechanism was provided by (Ansmann et al., 2019) using combined lidar and radar measurements over Cyprus. The authors found a close correspondence between predicted INP concentrations and observed ice crystal concentrations within Saharan dust-containing middle- and upper-tropospheric cloud layers. The investigated cirrus clouds formed at altitudes between 8 and 11 km and temperatures ranging from −35 to −57 °C, and in several cases the observed ice crystal concentrations could be fully explained by the available dust-derived INPs. Particularly noteworthy is the "dust-infused baroclinic storm" (DIBS) case described by the authors, in which a North African dust outbreak injected large quantities of Saharan dust into the upper troposphere. The resulting dust-enriched cirrus system could be tracked for more than 3,500 km from the Mediterranean to Central Asia, and the study concluded that mineral dust substantially contributed to the persistence and longevity of the cirrus cloud system. Similar dust-cirrus interactions were described in detail by other (Central) European studies (Seifert et al., 2023; Weger et al., 2018).

Comment: Sections 4.3 and 4.4 should be shortened.
Response: We agree. These sections have been condensed, while greater emphasis is now placed on unresolved questions concerning the combined effects of dust, atmospheric dynamics, and upper-tropospheric thermodynamic conditions.

We thank Reviewer 1 again for the constructive suggestions. In particular, the new vertically resolved dust analysis and the revised treatment of cirrus microphysics and atmospheric dynamics have substantially strengthened the manuscript.

Response to Reviewer 2

We thank Reviewer 2 for the critical and constructive assessment. The comments prompted substantial revisions to the statistical framework, reproducibility of the analysis, vertical characterization of dust, and interpretation of the results. Most importantly, we no longer claim a uniform strengthening of the dust–cirrus relationship over 2001–2025. Instead, the revised manuscript describes a persistent but temporally and seasonally variable association, with the clearest temporal change occurring in cirrus optical properties under high springtime dust loading.

1. Presentation

Comment: The main-text tables are excessively large and obscure the key findings.
Response: We agree. The tables have been substantially simplified, and the principal results are now emphasized graphically. Excessive numerical detail has been removed from the main text.

2. Reproducibility

Comment on the GAM inputs and geographic domain (insufficiently described)
Response: We agree. The revised Methods now explicitly define the study domain (Hungary), spatial averaging, event windows, predictor and response variables, and statistical procedures, allowing the analysis to be reproduced.

The study focuses on Hungary, located in the Carpathian Basin, Central Europe (all of the analyses were conducted using the shapefile defining the national borders). Due to its geographical location, the region is situated at the intersection of several major atmospheric circulation systems, where Atlantic, Mediterranean, and continental influences all play important roles. The basin-like topography favours the accumulation of air masses associated with long-range aerosol transport and provides favourable conditions for the formation and persistence of high-level cloud systems. The region is particularly sensitive to Saharan dust intrusions, which occur most frequently and intensely during the spring and summer seasons.

The new statistical analyses:

2.4. Event-based statistical analysis

To investigate whether the cloud properties associated with Saharan dust events depend on the presence of mineral dust at cirrus-relevant altitudes, an event-based analysis was performed using the 276 independently identified SDE days. Rather than relying primarily on correlations between dust concentration and individual cloud parameters, the analysis was designed to compare cloud states associated with SDEs against low-dust background conditions. Low-dust reference days were defined as non-SDE days for which the total-column dust mass remained below the 75th percentile (upper quartile) of the complete 2001–2025

daily dust distribution. This criterion yielded 6836 reference days and excluded the upper quartile of the total-column dust distribution, where substantial dust influence was more likely. All comparisons were performed separately for winter, spring, summer, and autumn to account for the pronounced seasonal variability in both Saharan dust transport and cloud conditions.

To examine whether the vertical penetration of dust into the upper troposphere was associated with the magnitude of the cloud response, SDEs were additionally divided within each season according to their Dust7–12 values. Events below or equal to the seasonal median Dust7–12 concentration were classified as lower-upper-tropospheric-dust SDEs, whereas events above the seasonal median were classified as higher-upper-tropospheric-dust SDEs. The use of season-specific thresholds avoided applying a single concentration criterion to seasons characterized by substantially different upper-tropospheric dust distributions. Three complementary contrasts were then evaluated: (i) all SDE days versus low-dust reference days, (ii) lower- and higher-Dust7–12 SDE subsets separately versus the corresponding seasonal reference, and (iii) higher- versus lower-Dust7–12 SDEs directly. The latter comparison was used to determine whether cloud properties differed systematically among SDEs depending on the amount of mineral dust present at 7–12 km.

The analysis included cirrus reflectance, effective ice particle radius, low-, mid-, and high-level cloud fraction, cloud-top pressure, cloud-top temperature, and OLR. Because several variables exhibited non-normal distributions and unequal group sizes, group differences were evaluated using two-sided Mann–Whitney U tests. The magnitude and direction of the differences were quantified using rank-biserial correlation (rrb) as a non-parametric effect-size measure, with positive values indicating higher values in the first group and negative values indicating lower values. To control for multiple comparisons, p-values were adjusted using the Benjamini–Hochberg false discovery rate (FDR) procedure, with FDR-adjusted ($q<0.05$) considered statistically significant. Group medians were used to characterize the magnitude of the observed differences.

Because vertically resolved Dust7–12 data were available only for the 276 SDE days, upper-tropospheric dust concentrations could not be directly compared between SDE and reference days. Accordingly, the low-dust reference group was defined independently using total-column dust mass, whereas Dust7–12 was used specifically to stratify the SDE population according to the degree of upper-tropospheric dust presence. This design therefore tests whether the cloud state associated with SDEs differs from low-dust background conditions and, more specifically, whether these anomalies become more pronounced when larger amounts of mineral dust are present at cirrus-relevant altitudes.

Comment: Given the global coverage of the datasets, the regional restriction should be justified and a broader/global analysis considered.

Response: We have clarified that the study is intentionally regional and event-based, focusing on Hungary, and independently identified Saharan dust events affecting Hungary. A global analysis would address a substantially different research question and is beyond the scope of the present study. We now state this limitation more clearly.

3. Statistical significance and validity

Comment on the cumulative dust-threshold means, what are not independent and should not be used as GAM inputs. Statistical inference should instead be performed at the daily/event level and account for temporal dependence.
Response: We agree with this important criticism. The statistical analysis has been rebuilt using daily observations within independently defined SDE windows rather than cumulative threshold averages. Overlapping event windows were resolved to avoid duplicate observations, and the revised Methods now clearly distinguish descriptive threshold analyses from inferential statistics.

Comment on the high R^2 values (very small p-values may result from pseudo-replication among cumulative thresholds)
Response: We agree. Therefore, cumulative threshold means are no longer used for statistical inference. They are retained only as descriptive summaries, while significance testing is based on the underlying daily/event-level observations.

4. Causality versus correlation

Comment: Besides the significance issue, even with signficant correlations, dust transport and cirrus may well just share external controls such as circulation and upper- tropospheric humidity. Changes in synoptic weather regimes could therefore increase both transported dust and cirrus without any change in the causal effect of dust.
Response: We agree and have revised the manuscript throughout to avoid unsupported causal language. The results are now described as dust–cloud associations, and we explicitly state that the observational analysis does not establish causality.
The revised Discussion explicitly considers circulation, vertical motion, wind shear, turbulence, and ice supersaturation as potential common controls. We therefore interpret the observed relationships as potentially reflecting combined aerosol, thermodynamic, and dynamical influences rather than a dust effect alone.

4.2. Evidence for changing dust–cloud relationships

The combined results indicate that the relationship between Saharan dust and upper-level cloud properties over Hungary has evolved during the past 25 years, although this evolution cannot be described as a uniform strengthening across all investigated variables. The clearest long-term change was found in cirrus reflectance, for which the SDE-associated anomaly increased substantially between the beginning and the end of the study period. Together with the increasing frequency of SDEs, this suggests that the long-term evolution involves both more frequent dust intrusions and changes in the optical properties of cirrus associated with high dust loading.
The consistency of the event-based comparisons strengthens this interpretation. SDEs with higher upper-tropospheric dust abundance showed more pronounced differences in several cloud properties not only relative to low-dust background conditions, but also relative to SDEs with lower Dust7–12 concentrations. This distinction is important because the latter comparison is restricted entirely to independently identified Saharan dust events and therefore specifically addresses differences associated with the amount of dust reaching

cirrus-relevant altitudes. The strongest and most coherent contrasts occurred in winter and spring, while their magnitude and the affected cloud properties varied among seasons. The pronounced seasonal dependence, particularly the coherent response observed in spring, further suggests that the effect associated with dust depends on the thermodynamic state of the atmosphere. Mineral dust can provide efficient ice-nucleating particles, but its influence on cirrus formation requires favourable temperature and ice-supersaturation conditions. Enhanced cirrus reflectance is therefore physically consistent with dust-related modification of ice-cloud formation. However, the weak and seasonally inconsistent response of effective ice particle radius does not provide sufficient evidence for a specific microphysical pathway, and heterogeneous ice nucleation should be regarded as a plausible interpretation rather than a directly demonstrated mechanism.
An important limitation is that Saharan dust transport and cloud formation are both closely linked to synoptic meteorological conditions. Moisture transport, vertical motion, temperature, and upper-tropospheric humidity may therefore contribute to the observed associations. Consequently, the results demonstrate a robust dust–cloud association, but do not establish causality. Long-term changes in the occurrence of conditions favourable for ice supersaturation could also contribute to a possible strengthening cirrus response, although such conditions were not directly quantified in this study.

Comment: This possibility is alluded to in the conclusion and in Sect. 4.2, but simple tests (e.g., including meteorological variables in the GAM) are not performed.
Response: We agree with the underlying concern. Rather than interpreting the statistical relationships as causal effects after meteorological adjustment, we have substantially narrowed the scope of our conclusions and explicitly discuss meteorological covariability as a limitation. A rigorous attribution of aerosol and dynamical effects would require additional upper-tropospheric dynamical and thermodynamic diagnostics and is beyond the scope of the present analysis.

Comment: Moreover, the chosen dust predictor is questionable. Total-column dust mass does not show whether dust is present at cirrus altitude or spatially collocated with the cloud.
Response: We fully agree and addressed this directly with a new vertically resolved MERRA-2 analysis. Dust exceeding 10^{-9} kg kg^{-1} was present at 7–12 km during 95.7% of the 276 SDEs, demonstrating frequent vertical co-occurrence of Saharan dust and cirrus-relevant altitudes. We additionally compared total-column and upper-tropospheric dust. Dust mass mixing ratios at 7–12 km showed stronger associations with several upper-level cloud properties than total-column dust loading, supporting the relevance of the vertically resolved dust metric.

Methods:
The threshold-based analysis extends this approach by progressively selecting days exceeding different column-dust levels, thereby characterizing dust-load-dependent cloud responses and their evolution across consecutive five-year periods without relying on a single arbitrary dusty-day threshold. Finally, vertically resolved MERRA-2 dust mass mixing ratios at 7–12 km were used to determine whether mineral dust was actually present at cirrus-relevant altitudes and whether cloud properties were more closely associated with upper-tropospheric

dust than with total-column loading. Thus, these metrics address complementary aspects of the problem—event occurrence, total dust burden, dust-load dependence, and vertical dust–cloud co-occurrence—rather than representing alternative definitions of the same quantity.
(…)
To assess whether Saharan dust was present at altitudes relevant to cirrus formation, the total-column analysis was complemented with three-dimensional MERRA-2 aerosol fields. For each of the identified SDEs, 3-hourly dust mass mixing ratios for the five MERRA-2 dust size bins (DU001–DU005) were extracted over the study domain from the native model-level aerosol product. Total dust mass mixing ratio (kg kg^{-1}) was calculated as the sum of the five size bins. Aerosol fields were matched to the corresponding three-dimensional MERRA-2 atmospheric fields, and the geometric height assigned to each model level was used to determine the actual altitude of the dust at every time step and grid point. This allowed the dust distribution to be evaluated independently of fixed model-level or pressure-level assumptions. Upper-tropospheric dust was primarily characterized over the 7–12 km altitude range, with additional calculations for the 7–8, 8–9, 9–10, and 10–12 km layers to examine the vertical dependence of the dust–cirrus relationship. Event-level mean dust mass mixing ratios were calculated from all grid points and 3-hourly time steps falling within each altitude interval. These vertically resolved dust metrics were subsequently compared with the MODIS and HIRS cloud properties used in the original analysis to determine whether cirrus responses were more closely associated with dust present at cirrus-relevant altitudes than with total-column dust loading.
(…)
To examine whether the vertical penetration of dust into the upper troposphere was associated with the magnitude of the cloud response, SDEs were additionally divided within each season according to their Dust7–12 values. Events below or equal to the seasonal median Dust7–12 concentration were classified as lower-upper-tropospheric-dust SDEs, whereas events above the seasonal median were classified as higher-upper-tropospheric-dust SDEs. The use of season-specific thresholds avoided applying a single concentration criterion to seasons characterized by substantially different upper-tropospheric dust distributions. Three complementary contrasts were then evaluated: (i) all SDE days versus low-dust reference days, (ii) lower- and higher-Dust7–12 SDE subsets separately versus the corresponding seasonal reference, and (iii) higher- versus lower-Dust7–12 SDEs directly. The latter comparison was used to determine whether cloud properties differed systematically among SDEs depending on the amount of mineral dust present at 7–12 km.

Results

3.2.2. Upper-tropospheric dust occurrence and comparison with column dust loading

The vertically resolved MERRA-2 analysis showed that mineral dust was frequently present at cirrus-relevant altitudes during the identified SDEs. Across the 276 events, the median event-mean dust mass mixing ratio in the 7–12 km layer was 9.63×10^{-8} kg kg^{-1} (Figure 3). Upper-tropospheric dust was not restricted to the lower part of this altitude range: the corresponding median was 8.33×10^{-9} kg kg^{-1} at 8–12 km and 4.37×10^{-9} kg kg^{-1} at 10–12 km. Of all SDEs, 264 (95.7%) exhibited event-mean dust mass mixing ratios exceeding 10^{-9} kg kg^{-1} between 7 and 12 km, while 204 (73.9%) exceeded 5×10^{-9} kg kg^{-1}, and 134 (48.6%) exceeded 10^{-8} kg kg^{-1}. Even when the analysis was restricted to 8–12 km, these thresholds were

exceeded in 93.1%, 67.0%, and 44.6% of the events, respectively. At 10–12 km, 81.2% of the SDEs still exceeded 10^{-9} kg kg^{-1}.
The amount of dust at 7–12 km was also substantial relative to that at 3–7 km; the upper-tropospheric mean reached at least 30% of the 3–7 km value in 62% of the events and at least 50% in 35.5% of the events. These results demonstrate that, within MERRA-2, Saharan dust during the investigated events was generally not confined to the lower and middle troposphere but frequently extended into the altitude range occupied by upper-level ice clouds.

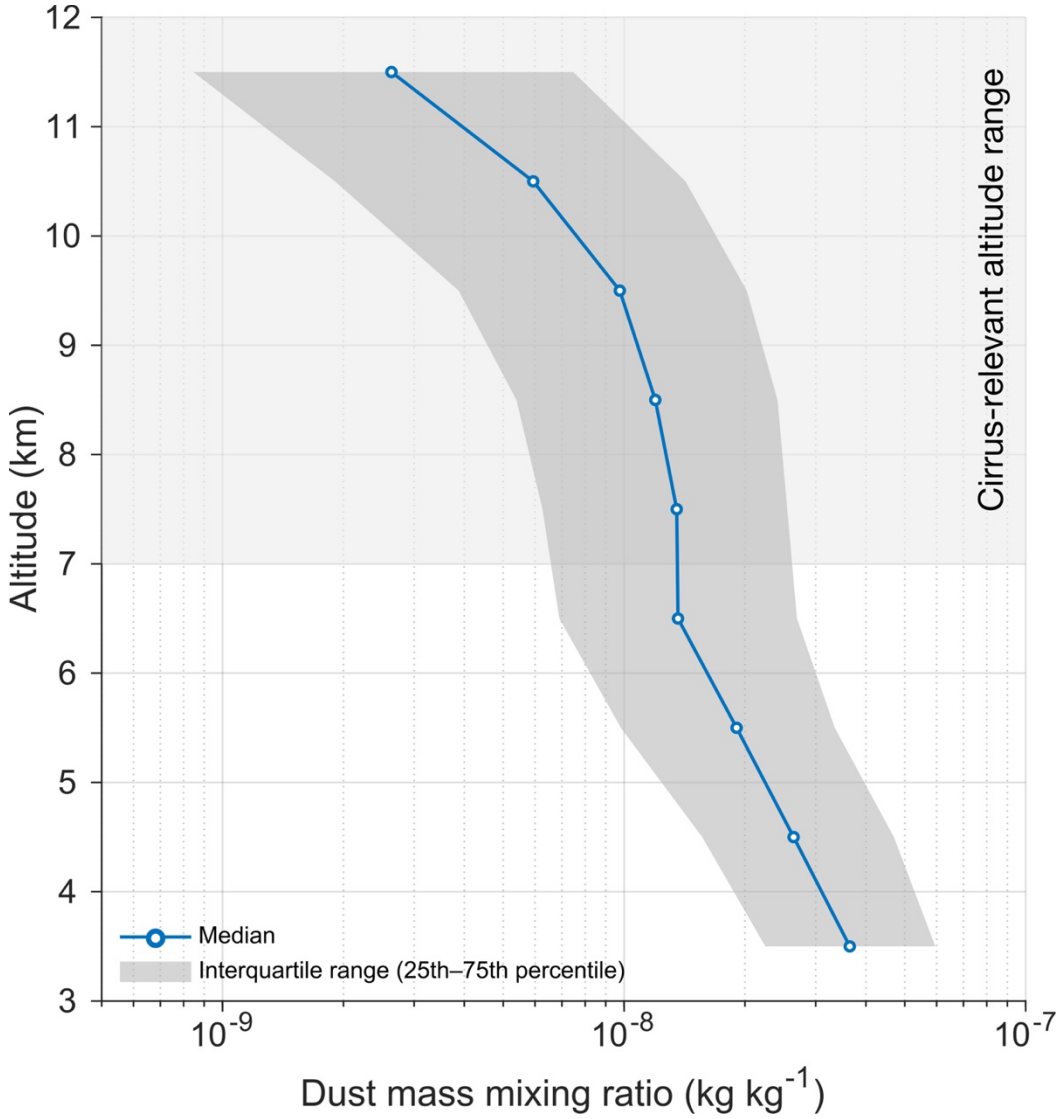

Figure 3. Vertical distribution of Saharan dust during the 276 identified SDEs. (The line shows the median MERRA-2 dust mass mixing ratio, with the shaded envelope representing the interquartile range, while the shaded 7–12 km layer indicates cirrus-relevant altitudes.)

We agree that the original wording of the manuscript on the strengthening response was too strong. The revised manuscript no longer claims a uniform or monotonic strengthening of the dust–cirrus relationship. Instead, our results indicate a persistent but temporally evolving relationship, with the clearest change found under extreme spring dust loading: median

cirrus reflectance increased from 0.075 in 2001–2005 to 0.186 in 2021–2025, while the fraction of extreme dust days simultaneously exhibiting extreme cirrus reflectance increased from 15.6% to 47.6%. These changes were non-monotonic across the intermediate periods and are now described accordingly.

We thank Reviewer 2 for identifying these important limitations. The revised manuscript now uses daily/event-level inference, explicitly evaluates dust at cirrus-relevant altitudes, provides clearer methodological information, and substantially reduces causal interpretation. We believe these changes have resulted in a more reproducible analysis and a more appropriately constrained interpretation of the observed dust–cirrus relationships.

Response to Community Comments by Daniel Williams, Iarla Boyce, Christos Mistios, Julia Canet

We thank the reviewers for their careful and constructive assessment. The comments are highly relevant and largely consistent with concerns raised during the interactive review. The manuscript has been substantially revised accordingly, particularly regarding causal interpretation, vertically resolved dust information, statistical analysis, and the interpretation of long-term changes.

RE: General comments

1. The GAM analysis indicates that the relationship between dust loading and cloud properties varies with time. This is evidence for non-stationarity of the statistical association, not necessarily that the physical response of clouds to dust has strengthened. An alternative explanation may be that the meteorological conditions associated with Saharan dust transport could have changed. The manuscript should therefore distinguish between a changing dust-cloud association and a strengthening of the causal influence of dust on cirrus formation.

Response: We fully agree. The manuscript has been revised throughout to distinguish statistical association from causal influence. We no longer claim a uniform strengthening of the physical dust effect. Instead, the results are described as a persistent but temporally evolving and non-monotonic dust–cirrus association, with the clearest temporal change occurring in cirrus optical properties under high springtime dust loading.

Results:

3.3. Long-term trends of dust and cirrus cloud relationships in spring

Based on the seasonal analysis above, the long-term assessment was focused on spring, which combined the largest number of identified SDEs and the highest mean dust loading

with the most coherent dust-dependent responses across cirrus reflectance, high-cloud fraction, cloud-top properties, and OLR.

The five-year analysis revealed substantial temporal variability in springtime SDE-associated cloud properties without a corresponding monotonic increase in upper-tropospheric dust loading. Median Dust7–12 during spring SDEs varied between 6.73×10^{-8} and 1.29×10^{-7} kg kg^{-1}, with the lowest value occurring in 2016–2020 and no systematic increase towards the end of the record. In contrast, the cirrus reflectance anomaly during high-Dust7–12 SDEs increased markedly: relative to the corresponding low-dust background, median cirrus reflectance was 143% higher in 2001–2005, 147% in 2006–2010, 318% in 2011–2015, 327% in 2016–2020, and 398% in 2021–2025. The absolute median cirrus reflectance increased from 0.116 in 2001–2005 to 0.223 in 2021–2025, while the corresponding background values remained similar (0.048 and 0.045, respectively).

Other cloud properties showed persistent but less monotonic differences. High-cloud fraction during high-Dust7–12 SDEs was 122–161% above background during 2001–2015, 54% higher in 2016–2020, and 135% higher in 2021–2025. Cloud-top pressure remained 25–34% lower and cloud-top temperature approximately 5–7% lower than background throughout the five periods, with the largest recent differences occurring in 2021–2025. Effective ice particle radius showed greater temporal variability: the anomaly changed from +2.8% in 2001–2005 to −15.7% in 2006–2010, −8.3% in 2011–2015, approximately zero in 2016–2020, and −7.7% in 2021–2025. OLR remained lower during high-Dust7–12 SDEs in every period, with differences ranging from approximately −10% to −17%. Thus, among the investigated variables, the clearest five-year change was observed in cirrus reflectance, whose SDE-associated enhancement became substantially larger over the study period despite the absence of a parallel increase in Dust7–12.

As a complementary analysis independent of the vertically resolved SDE stratification, the longer-term behaviour was also examined using progressively restrictive total-column dust-loading thresholds applied to the complete daily dataset (Figure 4). Middle- and high-level cloud cover fractions generally increase with increasing dust column mass density, whereas low-cloud fraction shows neither a consistent dust-load dependence nor a systematic temporal pattern. The relationship is most pronounced for high clouds, for which higher dust-loading thresholds are associated with larger cloud fractions in nearly all five-year periods. Differences among the periods are also evident, with the largest high-cloud fractions occurring under the highest dust-loading conditions in the later part of the record. During 2021–2025, high-cloud fractions associated with the highest dust loads were approximately 1.5 times those observed during 2001–2005.

Conclusions:

The event-based analysis of 276 independently identified Saharan dust events provided further evidence for a systematic dust–cirrus association. SDEs were characterized by significantly enhanced cirrus reflectance and high-cloud fraction and by higher and colder cloud tops, with the most coherent response occurring in spring. These patterns were consistently supported by event–background comparisons, effect-size estimates, and direct comparisons between SDEs with lower and higher upper-tropospheric dust concentrations. The vertically resolved analysis showed that the strongest cloud anomalies occurred during SDEs with enhanced mineral dust concentrations at 7–12 km. Relative to low-dust reference conditions, high-Dust7–12 SDEs were characterized by substantially greater cirrus reflectance

and high-cloud fraction and by higher and colder cloud tops in all seasons. The response was particularly coherent in spring, when cirrus reflectance and high-cloud fraction were 272% and 133% higher, respectively, while effective ice particle radius was 7.2% smaller and OLR 14.4% lower than under low-dust conditions. The direct comparison between SDE subsets further showed significantly smaller ice particle radii during high- than during low-Dust7–12 spring events.
The five-year springtime analysis further revealed that these cloud changes were not accompanied by a monotonic increase in upper-tropospheric dust loading. Instead, the relative cirrus-reflectance enhancement during high-Dust7–12 SDEs increased from 143% in 2001–2005 to 398% in 2021–2025, whereas high-cloud fraction and cloud-top properties showed persistent but non-monotonic anomalies and effective ice particle radius exhibited greater temporal variability. Collectively, the results indicate increasingly frequent Saharan dust intrusions and a more pronounced springtime cirrus optical response during SDEs containing substantial dust at cirrus-relevant altitudes, rather than a uniform strengthening across all investigated cloud and radiative properties.

2. On non-independence of cumulative dust thresholds and interpretation of R^2

Response: We agree. Cumulative threshold subsets are nested and therefore non-independent. In the revised manuscript, these threshold curves are used only descriptively and not for statistical inference. The main inferential analysis has been replaced by an event-based framework using the underlying observations. We have also removed the interpretation that high model R^2 values demonstrate the fraction of cloud variability explained specifically by dust loading.

Beyond the analysis of discrete dust events, the relationship between atmospheric dust loading and cloud properties was investigated using continuous dust column mass density thresholds. In this approach, progressively restrictive dust-loading thresholds were applied. Because no universally accepted threshold exists for distinguishing dusty and non-dusty conditions across different geographical and climatic environments, and seasons, multiple dust-loading thresholds were applied. Dust column mass density threshold values were systematically varied between 0 and 0.006 g m^{-2} in increments of 0.0001 g m^{-2}. For each threshold value, daily mean cloud parameters, including cirrus reflectance, high cloud cover fraction, and effective ice particle radius, were calculated and subsequently analysed seasonally within consecutive five-year time windows across the 2001–2025 study period. This approach enabled the assessment of how different dust-loading regimes are associated with changes in the optical and spatial characteristics of cirrus clouds. To evaluate radiative impacts, the same methodology was applied to ice cloud effective particle radius, cloud fractions (at different heights), outgoing longwave radiation (OLR) data, allowing the investigation of long-term relationships between atmospheric dust loading, cirrus cloud development, and upper-tropospheric radiative processes. While this total-column threshold analysis provides a complementary view of dust-load-dependent cloud variability over the full daily record, the event-based analysis described below focuses specifically on the 276 independently identified SDEs and uses vertically resolved dust information to assess whether mineral dust was present at cirrus-relevant altitudes.

3. On the temporal autocorrelation

Response: We agree that temporal autocorrelation may remain within the daily observations, particularly during persistent multi-day meteorological conditions. We have not explicitly modelled residual autocorrelation in the present analysis and now acknowledge this as a limitation. Importantly, the original GAM-based interpretation has been substantially reduced, and the main conclusions are now based primarily on event-based non-parametric comparisons. Nevertheless, some temporal dependence may remain, and we therefore interpret statistical significance cautiously and explicitly identify this issue as a limitation of the present observational framework.

4. On total-column dust versus dust at cirrus altitude

Response: We fully agree and have addressed this with a new vertically resolved MERRA-2 analysis. Across the 276 SDEs, 95.7% exhibited event-mean dust mass mixing ratios exceeding 10^{-9} kg kg^{-1} at 7–12 km. Additional analyses were performed for 8–12 and 10–12 km. Thus, the revised manuscript explicitly evaluates the presence of mineral dust at cirrus-relevant altitudes rather than relying solely on total-column dust loading.

Methods:
The threshold-based analysis extends this approach by progressively selecting days exceeding different column-dust levels, thereby characterizing dust-load-dependent cloud responses and their evolution across consecutive five-year periods without relying on a single arbitrary dusty-day threshold. Finally, vertically resolved MERRA-2 dust mass mixing ratios at 7–12 km were used to determine whether mineral dust was actually present at cirrus-relevant altitudes and whether cloud properties were more closely associated with upper-tropospheric dust than with total-column loading. Thus, these metrics address complementary aspects of the problem—event occurrence, total dust burden, dust-load dependence, and vertical dust–cloud co-occurrence—rather than representing alternative definitions of the same quantity.
(…)
To assess whether Saharan dust was present at altitudes relevant to cirrus formation, the total-column analysis was complemented with three-dimensional MERRA-2 aerosol fields. For each of the identified SDEs, 3-hourly dust mass mixing ratios for the five MERRA-2 dust size bins (DU001–DU005) were extracted over the study domain from the native model-level aerosol product. Total dust mass mixing ratio (kg kg^{-1}) was calculated as the sum of the five size bins. Aerosol fields were matched to the corresponding three-dimensional MERRA-2 atmospheric fields, and the geometric height assigned to each model level was used to determine the actual altitude of the dust at every time step and grid point. This allowed the dust distribution to be evaluated independently of fixed model-level or pressure-level assumptions. Upper-tropospheric dust was primarily characterized over the 7–12 km altitude range, with additional calculations for the 7–8, 8–9, 9–10, and 10–12 km layers to examine the vertical dependence of the dust–cirrus relationship. Event-level mean dust mass mixing ratios were calculated from all grid points and 3-hourly time steps falling within each altitude interval. These vertically resolved dust metrics were subsequently compared with the MODIS and HIRS cloud properties used in the original analysis to determine whether cirrus responses were more closely associated with dust present at cirrus-relevant altitudes than with total-column dust loading.
(…)

To examine whether the vertical penetration of dust into the upper troposphere was associated with the magnitude of the cloud response, SDEs were additionally divided within each season according to their Dust7–12 values. Events below or equal to the seasonal median Dust7–12 concentration were classified as lower-upper-tropospheric-dust SDEs, whereas events above the seasonal median were classified as higher-upper-tropospheric-dust SDEs. The use of season-specific thresholds avoided applying a single concentration criterion to seasons characterized by substantially different upper-tropospheric dust distributions. Three complementary contrasts were then evaluated: (i) all SDE days versus low-dust reference days, (ii) lower- and higher-Dust7–12 SDE subsets separately versus the corresponding seasonal reference, and (iii) higher- versus lower-Dust7–12 SDEs directly. The latter comparison was used to determine whether cloud properties differed systematically among SDEs depending on the amount of mineral dust present at 7–12 km.

Results

3.2.2. Upper-tropospheric dust occurrence and comparison with column dust loading

The vertically resolved MERRA-2 analysis showed that mineral dust was frequently present at cirrus-relevant altitudes during the identified SDEs. Across the 276 events, the median event-mean dust mass mixing ratio in the 7–12 km layer was 9.63×10^{-8} kg kg^{-1} (Figure 3). Upper-tropospheric dust was not restricted to the lower part of this altitude range: the corresponding median was 8.33×10^{-9} kg kg^{-1} at 8–12 km and 4.37×10^{-9} kg kg^{-1} at 10–12 km. Of all SDEs, 264 (95.7%) exhibited event-mean dust mass mixing ratios exceeding 10^{-9} kg kg^{-1} between 7 and 12 km, while 204 (73.9%) exceeded 5×10^{-9} kg kg^{-1}, and 134 (48.6%) exceeded 10^{-8} kg kg^{-1}. Even when the analysis was restricted to 8–12 km, these thresholds were exceeded in 93.1%, 67.0%, and 44.6% of the events, respectively. At 10–12 km, 81.2% of the SDEs still exceeded 10^{-9} kg kg^{-1}.

The amount of dust at 7–12 km was also substantial relative to that at 3–7 km; the upper-tropospheric mean reached at least 30% of the 3–7 km value in 62% of the events and at least 50% in 35.5% of the events. These results demonstrate that, within MERRA-2, Saharan dust during the investigated events was generally not confined to the lower and middle troposphere but frequently extended into the altitude range occupied by upper-level ice clouds.

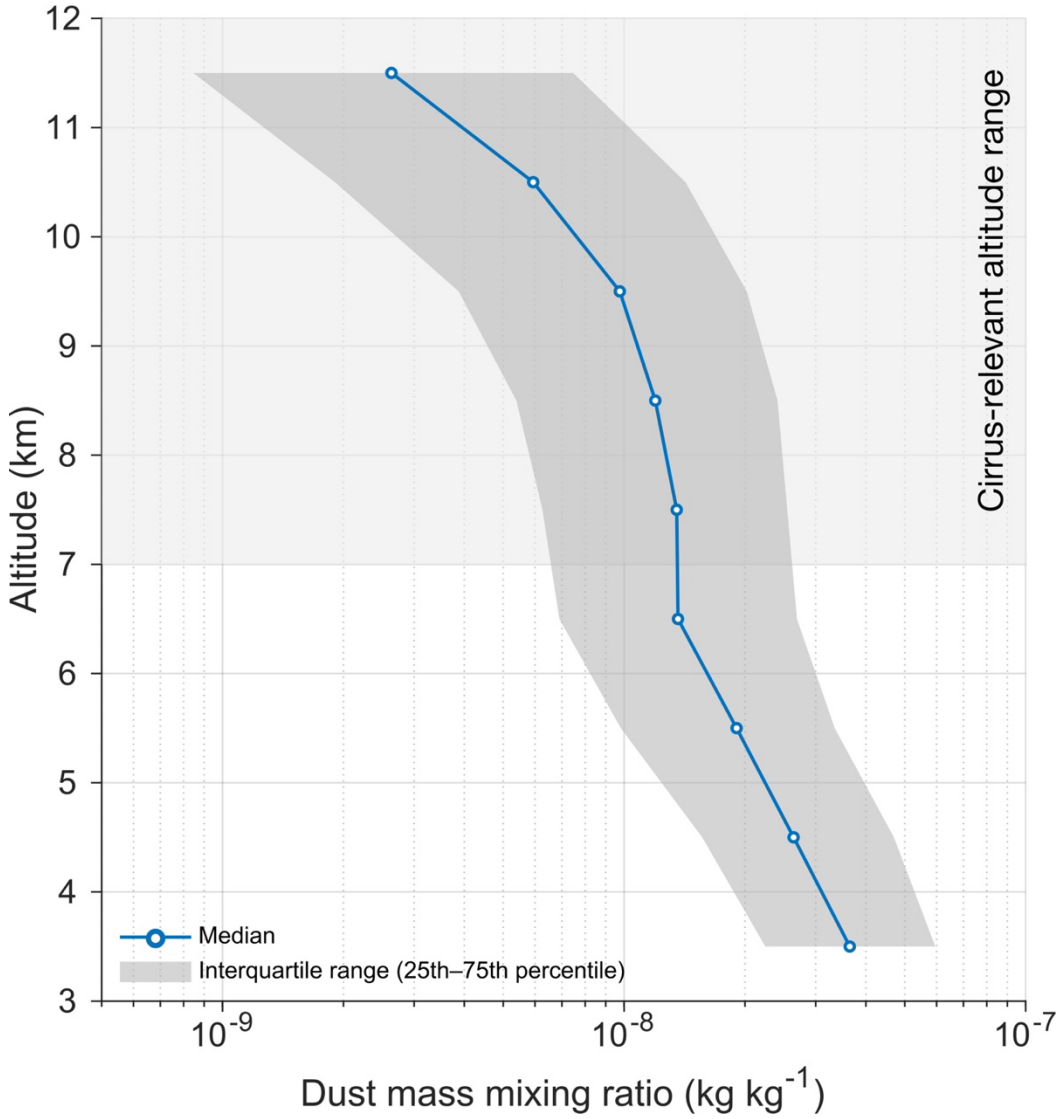

Figure 3. Vertical distribution of Saharan dust during the 276 identified SDEs. (The line shows the median MERRA-2 dust mass mixing ratio, with the shaded envelope representing the interquartile range, while the shaded 7–12 km layer indicates cirrus-relevant altitudes.)

5. Absolute versus relative number of high-reflectance events

Response: We agree. The revised analysis uses relative rather than absolute occurrence frequencies. For example, under extreme spring dust loading, the fraction of events simultaneously exhibiting extreme cirrus reflectance increased from 15.6% in 2001–2005 to 47.6% in 2021–2025. The intermediate periods also demonstrate that this evolution was non-monotonic.

3.3. Long-term trends of dust and cirrus cloud relationships in spring

Based on the seasonal analysis above, the long-term assessment was focused on spring, which combined the largest number of identified SDEs and the highest mean dust loading with the most coherent dust-dependent responses across cirrus reflectance, high-cloud fraction, cloud-top properties, and OLR.

The five-year analysis revealed substantial temporal variability in springtime SDE-associated cloud properties without a corresponding monotonic increase in upper-tropospheric dust loading. Median Dust7–12 during spring SDEs varied between 6.73×10^{-8} and 1.29×10^{-7} kg kg^{-1}, with the lowest value occurring in 2016–2020 and no systematic increase towards the end of the record. In contrast, the cirrus reflectance anomaly during high-Dust7–12 SDEs increased markedly: relative to the corresponding low-dust background, median cirrus reflectance was 143% higher in 2001–2005, 147% in 2006–2010, 318% in 2011–2015, 327% in 2016–2020, and 398% in 2021–2025. The absolute median cirrus reflectance increased from 0.116 in 2001–2005 to 0.223 in 2021–2025, while the corresponding background values remained similar (0.048 and 0.045, respectively).

Other cloud properties showed persistent but less monotonic differences. High-cloud fraction during high-Dust7–12 SDEs was 122–161% above background during 2001–2015, 54% higher in 2016–2020, and 135% higher in 2021–2025. Cloud-top pressure remained 25–34% lower and cloud-top temperature approximately 5–7% lower than background throughout the five periods, with the largest recent differences occurring in 2021–2025. Effective ice particle radius showed greater temporal variability: the anomaly changed from +2.8% in 2001–2005 to −15.7% in 2006–2010, −8.3% in 2011–2015, approximately zero in 2016–2020, and −7.7% in 2021–2025. OLR remained lower during high-Dust7–12 SDEs in every period, with differences ranging from approximately −10% to −17%. Thus, among the investigated variables, the clearest five-year change was observed in cirrus reflectance, whose SDE-associated enhancement became substantially larger over the study period despite the absence of a parallel increase in Dust7–12.

As a complementary analysis independent of the vertically resolved SDE stratification, the longer-term behaviour was also examined using progressively restrictive total-column dust-loading thresholds applied to the complete daily dataset (Figure 4). Middle- and high-level cloud cover fractions generally increase with increasing dust column mass density, whereas low-cloud fraction shows neither a consistent dust-load dependence nor a systematic temporal pattern. The relationship is most pronounced for high clouds, for which higher dust-loading thresholds are associated with larger cloud fractions in nearly all five-year periods. Differences among the periods are also evident, with the largest high-cloud fractions occurring under the highest dust-loading conditions in the later part of the record. During 2021–2025, high-cloud fractions associated with the highest dust loads were approximately 1.5 times those observed during 2001–2005.

Cloud-top pressure and cloud-top temperature also show marked variations across the dust-loading thresholds. Higher dust column mass densities are generally associated with lower cloud-top pressures and lower cloud-top temperatures, indicating a shift towards higher and colder cloud tops. These differences are particularly pronounced during 2011–2015 and 2021–2025. The simultaneous increase in high-cloud fraction and decrease in cloud-top pressure and temperature is therefore a consistent feature of the higher dust-loading subsets, although the magnitude of the response varies among the five-year periods.

The strongest dust-load-dependent changes among the cirrus-specific properties are observed for cirrus reflectance and effective ice-particle radius. In spring, cirrus reflectance increases towards higher dust-loading thresholds during all five-year periods, but both the magnitude and range of the response differ substantially among periods. The largest reflectance values at elevated dust loads occur during 2016–2020 and 2021–2025. Effective ice-particle radius shows an opposite pattern, with smaller values generally occurring at higher dust-loading thresholds. Thus, the highest dust-loading subsets are characterized by a

combination of enhanced cirrus reflectance and reduced effective ice-particle radius. As with the other cloud variables, however, the magnitude of these differences is not uniform across the five five-year periods.

6. Effective ice-particle radius

Response: We agree that differences of only a few micrometres should not be overinterpreted. The revised manuscript no longer uses these relatively small changes as evidence for a major long-term microphysical response. Effective-radius results are treated as secondary, while the main conclusions are based on the more robust changes in cirrus reflectance, high-cloud fraction, and cloud-top properties.
In the revised manuscript, we have therefore placed greater emphasis on the statistical robustness and seasonal consistency of the observed differences rather than interpreting small changes in effective radius as direct evidence of dust-induced ice nucleation.
Our revised event-based analysis indicates that statistically significant differences in effective ice-particle radius are primarily confined to spring. During springtime Saharan dust events characterized by high upper-tropospheric dust concentrations (Dust7–12), the median effective radius was 28.44 µm, compared with 30.65 µm under low-dust reference conditions, corresponding to a reduction of approximately 2.22 µm (7.2%; FDR-adjusted $q \approx 0.0012$). Importantly, a separate comparison restricted entirely to independently identified Saharan dust events also revealed a significant difference between high- and low-Dust7–12 conditions (28.44 versus 31.90 µm, respectively; $q \approx 0.0023$).
These two independent group comparisons provide statistical support for a springtime association between enhanced upper-tropospheric dust abundance and smaller retrieved ice-particle radii. However, statistical significance does not eliminate the systematic uncertainties inherent in satellite retrievals, and the observed differences should not be interpreted as precise measurements of dust-induced changes in ice-crystal size.

7. Interpretation of OLR

Response: We agree. The OLR discussion has been substantially moderated. We now explicitly state that the observed OLR variations cannot be uniquely attributed to dust-induced cirrus changes because temperature, humidity, cloud properties, and dust itself may contribute simultaneously. OLR is therefore interpreted as an integrated radiative signature associated with dust-loading conditions rather than as an isolated dust or cirrus radiative effect.

RE: Specific comments

1. Twomey (1974) deals with liquid-cloud-aerosol interactions. I would suggest removing this reference.
Response: We agree and have removed this reference from the discussion of ice-cloud aerosol interactions.

2. Homogeneous nucleation does not require INPs. The authors may want to distinguish between homogeneous and heterogeneous nucleation.

Response: We agree. The revised Introduction now clearly distinguishes homogeneous freezing, which does not require INPs, from heterogeneous ice nucleation involving INPs.

A central challenge in representing cirrus clouds in atmospheric models is the competition between homogeneous freezing and heterogeneous ice nucleation. Homogeneous freezing of solution droplets generally requires high ice supersaturation and can produce large numbers of ice crystals, whereas heterogeneous nucleation on ice-nucleating particles can initiate ice formation at lower supersaturation and modify the subsequent evolution of the cloud (Kärcher et al., 2022, 2023).
(…)
Mineral dust is particularly relevant in this context because it represents one of the most important atmospheric sources of ice-nucleating particles, although its activity depends strongly on particle concentration, mineralogical composition, temperature, and nucleation mode (DeMott et al., 2003, 2010; Niemand et al., 2012; Ullrich, 2017).

3. K-feldspart is a more efficient ice nucleator compared to calcite and quartz. Clarifying the relative efficiencies would improve the statement.
Response: Thank you. The text has been revised to clarify that K-feldspar is generally a more efficient ice-nucleating mineral component than quartz or calcite.

Mineral aerosol particles, especially those rich in K-feldspar, quartz and calcite, are known to act as highly efficient heterogeneous ice nuclei under the low-temperature conditions of the upper troposphere (Atkinson et al., 2013; Chatziparaschos et al., 2023; Harrison et al., 2019; Hoose et al., 2008; Hoose and Möhler, 2012; Seifert et al., 2010).

4. This statement could do with a citation. Varga (2020) is cited for a similar statement later in the manuscript.
Response: We agree. The appropriate reference has been added to support this statement.

5. Sample sizes should be reported across dust thresholds, seasons and five-year periods, particularly at the highest dust loadings where relatively few observations may control the inferred response.
Response: Sample sizes are now reported for the principal seasonal, event-based, and five-year comparisons, particularly where increasingly restrictive dust conditions reduce the number of observations.

6. If the +ε error term in the model assumes a Gaussian error, this may be inappropriate for several variables, e.g. effective radius and cloud fraction. I recommend the authors assess the residual distributions for each model and justify the use of a Gaussian family or clarify the use of an alternative family.
Response: We agree that a Gaussian assumption may not be appropriate for all variables. The original GAM-based inference has therefore been substantially de-emphasized and replaced by a non-parametric event-based analysis using Mann–Whitney U tests, rank-biserial effect sizes, and FDR correction. The principal statistical conclusions consequently do not rely on Gaussian residual assumptions.

7. Tables 1 and 3 are quite large and it is unclear what is supposed to be demonstrated by them. If a trend is being demonstrated a time-series figure may be more appropriate with the tables being moved to an appendix or supplementary material.
Response: We agree. The presentation has been substantially simplified, with the key temporal and dust-dependent relationships emphasized graphically and the main-text tables reduced to the most relevant results.

8. Table 3: it is not obvious what the column 'change %' is being calculated from. I presume it is the final minus first column, but this should be made more explicit
Response: Thank you. The definition of percentage change has been clarified in the corresponding table caption/text to explicitly state the reference against which the change is calculated.

Technical comments

1. Overall inconsistency in the use of units, with different notations used at times (e.g. ms^-1 versus m/s). Please correct; if using LaTeX the siunitx package can be very useful.
Response: Units and their notation have been checked and standardized throughout the manuscript.

2. Some acronyms are defined multiple times in the manuscript, particularly OLR.
Response: The manuscript has been checked and redundant definitions, including repeated definitions of OLR, have been removed.

3. Figure captions should be as explicit as possible. Even if you have a legend, you should still state that 'shaded bars represent X...', which is especially beneficial for those using assistive technology.
Response: Figure captions have been revised to be more self-contained and explicitly describe the meaning of lines, symbols, and shaded areas where applicable.

We thank the reviewers again for these constructive comments. The revised manuscript now more clearly distinguishes association from causation, directly evaluates dust at cirrus-relevant altitudes, uses an event-based non-parametric statistical framework, and adopts a substantially more cautious interpretation of the temporal, microphysical, and radiative results. We also explicitly acknowledge the remaining limitation associated with temporal dependence in the observational data.

Detailed description of the major changes in the manuscript

The Methods were completed:

Upper tropospheric dust

To assess whether Saharan dust was present at altitudes relevant to cirrus formation, the total-column analysis was complemented with three-dimensional MERRA-2 aerosol fields. For each of the identified SDEs, 3-hourly dust mass mixing ratios for the five MERRA-2 dust size bins (DU001–DU005) were extracted over the study domain from the native model-level aerosol product. Total dust mass mixing ratio (kg kg^{-1}) was calculated as the sum of the five size bins. Aerosol fields were matched to the corresponding three-dimensional MERRA-2 atmospheric fields, and the geometric height assigned to each model level was used to determine the actual altitude of the dust at every time step and grid point. This allowed the dust distribution to be evaluated independently of fixed model-level or pressure-level assumptions. Upper-tropospheric dust was primarily characterized over the 7–12 km altitude range, with additional calculations for the 7–8, 8–9, 9–10, and 10–12 km layers to examine the vertical dependence of the dust–cirrus relationship. Event-level mean dust mass mixing ratios were calculated from all grid points and 3-hourly time steps falling within each altitude interval. These vertically resolved dust metrics were subsequently compared with the MODIS and HIRS cloud properties used in the original analysis to determine whether cirrus responses were more closely associated with dust present at cirrus-relevant altitudes than with total-column dust loading.

Event-based statistical analysis

To investigate whether the cloud properties associated with Saharan dust events depend on the presence of mineral dust at cirrus-relevant altitudes, an event-based analysis was performed using the 276 independently identified SDE days. Rather than relying primarily on correlations between dust concentration and individual cloud parameters, the analysis was designed to compare cloud states associated with SDEs against low-dust background conditions. Low-dust reference days were defined as non-SDE days for which the total-column dust mass remained below the 75th percentile (upper quartile) of the complete 2001–2025 daily dust distribution. This criterion yielded 6836 reference days and excluded the upper quartile of the total-column dust distribution, where substantial dust influence was more likely. All comparisons were performed separately for winter, spring, summer, and autumn to account for the pronounced seasonal variability in both Saharan dust transport and cloud conditions.

To examine whether the vertical penetration of dust into the upper troposphere was associated with the magnitude of the cloud response, SDEs were additionally divided within each season according to their Dust7–12 values. Events below or equal to the seasonal median Dust7–12 concentration were classified as lower-upper-tropospheric-dust SDEs, whereas events above the seasonal median were classified as higher-upper-tropospheric-dust SDEs. The use of season-specific thresholds avoided applying a single concentration criterion to seasons characterized by substantially different upper-tropospheric dust distributions. Three complementary contrasts were then evaluated: (i) all SDE days versus low-dust reference days, (ii) lower- and higher-Dust7–12 SDE subsets separately versus the corresponding seasonal reference, and (iii) higher- versus lower-Dust7–12 SDEs directly. The latter comparison was used to determine whether cloud properties differed systematically among SDEs depending on the amount of mineral dust present at 7–12 km.

The analysis included cirrus reflectance, effective ice particle radius, low-, mid-, and high-level cloud fraction, cloud-top pressure, cloud-top temperature, and outgoing longwave radiation (OLR). Because several variables exhibited non-normal distributions and unequal group sizes, group differences were evaluated using two-sided Mann–Whitney U tests. The magnitude and direction of the differences were quantified using rank-biserial correlation (rrb) as a non-parametric effect-size measure, with positive values indicating higher values in the first group and negative values indicating lower values. To control for multiple comparisons, p-values were adjusted using the Benjamini–Hochberg false discovery rate (FDR) procedure, with FDR-adjusted ($q<0.05$) considered statistically significant. Group medians were used to characterize the magnitude of the observed differences.
Because vertically resolved Dust7–12 data were available only for the 276 SDE days, upper-tropospheric dust concentrations could not be directly compared between SDE and reference days. Accordingly, the low-dust reference group was defined independently using total-column dust mass, whereas Dust7–12 was used specifically to stratify the SDE population according to the degree of upper-tropospheric dust presence. This design therefore tests whether the cloud state associated with SDEs differs from low-dust background conditions and, more specifically, whether these anomalies become more pronounced when larger amounts of mineral dust are present at cirrus-relevant altitudes.

New findings have been added to the results:

Upper-tropospheric dust occurrence and comparison with column dust loading

The vertically resolved MERRA-2 analysis showed that mineral dust was frequently present at cirrus-relevant altitudes during the identified SDEs. Across the 276 events, the median event-mean dust mass mixing ratio in the 7–12 km layer was 9.63×10^{-8} kg kg^{-1} (Figure 3). Upper-tropospheric dust was not restricted to the lower part of this altitude range: the corresponding median was 8.33×10^{-9} kg kg^{-1} at 8–12 km and 4.37×10^{-9} kg kg^{-1} at 10–12 km. Of all SDEs, 264 (95.7%) exhibited event-mean dust mass mixing ratios exceeding 10^{-9} kg kg^{-1} between 7 and 12 km, while 204 (73.9%) exceeded 5×10^{-9} kg kg^{-1}, and 134 (48.6%) exceeded 10^{-8} kg kg^{-1}. Even when the analysis was restricted to 8–12 km, these thresholds were exceeded in 93.1%, 67.0%, and 44.6% of the events, respectively. At 10–12 km, 81.2% of the SDEs still exceeded 10^{-9} kg kg^{-1}.
The amount of dust at 7–12 km was also substantial relative to that at 3–7 km; the upper-tropospheric mean reached at least 30% of the 3–7 km value in 62% of the events and at least 50% in 35.5% of the events. These results demonstrate that, within MERRA-2, Saharan dust during the investigated events was generally not confined to the lower and middle troposphere but frequently extended into the altitude range occupied by upper-level ice clouds.

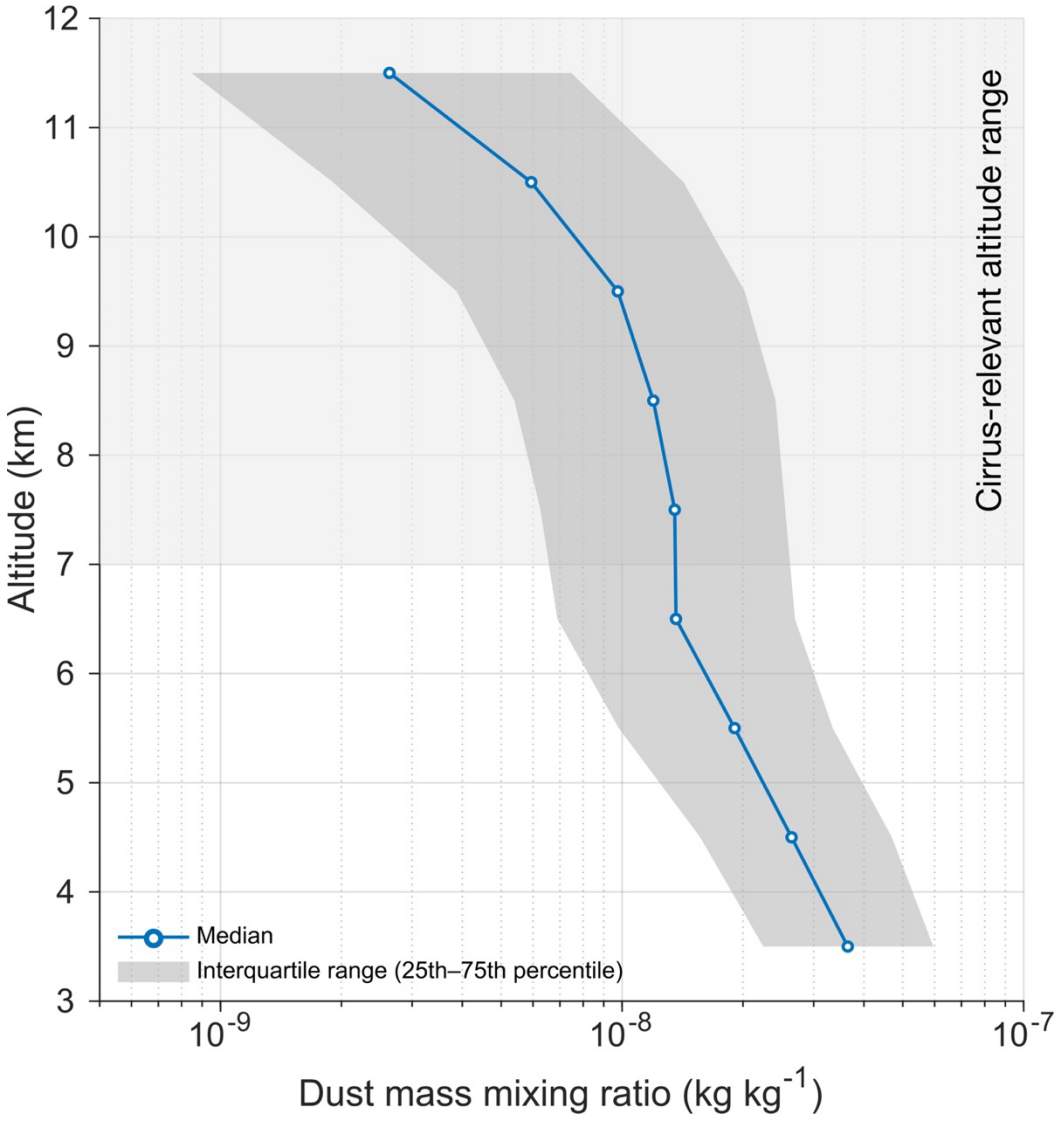

Figure 3. Vertical distribution of Saharan dust during the 276 identified SDEs. (The line shows the median MERRA-2 dust mass mixing ratio, with the shaded envelope representing the interquartile range, while the shaded 7–12 km layer indicates cirrus-relevant altitudes.)

Seasonal cloud-property differences associated with upper-tropospheric dust during SDEs

The event-based analysis revealed pronounced seasonal differences in cloud and radiative properties between Saharan dust events and low-dust reference conditions (Table 2). The differences were particularly marked for SDEs characterized by above-median dust concentrations in the 7–12 km layer. Across all seasons, these high-Dust7–12 events were associated with significantly enhanced cirrus reflectance and high-cloud fraction, together with substantially lower cloud-top pressure and temperature. Most of these differences remained highly significant after FDR correction and were accompanied by moderate to large rank-biserial effect sizes.

The largest overall contrasts were observed during winter and spring. In winter, high-Dust7–12 SDEs showed particularly large differences in high-cloud fraction, cloud-top properties, and OLR relative to low-dust reference conditions. Spring exhibited a similarly coherent pattern, with enhanced cirrus reflectance and high-cloud fraction and reduced cloud-top pressure, cloud-top temperature, and OLR. A significant reduction in effective ice particle

radius was also detected in spring, whereas particle-size differences were not statistically significant in the other seasons. Summer exhibited smaller cirrus and radiative differences, although high-cloud fraction and cloud-top properties remained significantly different from reference conditions. During autumn, the largest differences were observed in high-cloud fraction and cloud-top pressure and temperature.

Direct comparison of SDEs with above- and below-median Dust7–12 concentrations showed that the differences were not restricted to the contrast between SDE and reference conditions. Higher upper-tropospheric dust concentrations within SDEs were accompanied by significantly greater cirrus reflectance and high-cloud fraction during winter and spring. Spring high-Dust7–12 events additionally showed significantly smaller effective ice particle radii and lower OLR than lower-Dust7–12 events. During summer, the most pronounced within-SDE difference occurred in high-cloud fraction, whereas autumn showed the clearest differences in cloud-top pressure and temperature. Thus, the seasonal analysis identified distinct cloud-property differences not only between SDEs and low-dust background conditions but also according to the amount of mineral dust present within the 7–12 km layer during the events.

Table 2. Relative changes in cloud and radiative properties during high-Dust7–12 SDEs compared with low-dust reference conditions.

Season	Cirrus reflectance	High cloud fraction	Effective ice cloud radius	Cloud top pressure	Cloud top temperature	OLR
Winter	+194.5%***	+146.5%***	−4.9% n.s.	−44.0%***	−8.8%***	−16.1%***
Spring	+272.0%***	+133.2%***	−7.2%**	−30.0%***	−5.5%***	−14.4%***
Summer	+99.3%***	+94.7%***	0.0% n.s.	−34.8%***	−6.6%***	−4.6%*
Autumn	+160.9%***	+119.7%***	−4.8% n.s.	−41.4%***	−7.2%***	−8.6%*

Values represent percentage differences between median cloud properties during SDEs with above-seasonal-median Dust7–12 concentrations and the corresponding low-dust reference conditions, calculated relative to the reference median. Statistical significance is based on two-sided Mann–Whitney U tests with Benjamini–Hochberg FDR correction: *q<0.05, **q<0.01, ***q<0.001; n.s., not significant.

A separate within-SDE comparison was performed to determine whether cloud properties differed according to upper-tropospheric dust abundance independently of the SDE–background contrast. For this analysis, SDEs with above-seasonal-median Dust7–12 concentrations were compared directly with SDEs below or equal to the corresponding seasonal median.

In winter, median cirrus reflectance was 0.183 in the higher-Dust7–12 group compared with 0.068 in the lower-Dust7–12 group, while high-cloud fraction was 0.810 and 0.610, respectively. Cloud-top temperature decreased from 233.9 to 223.8 K and OLR from 199.9 to 172.0 W m^{-2}; all four differences remained significant after FDR correction. In spring, cirrus reflectance increased from 0.079 to 0.167 and high-cloud fraction from 0.565 to 0.708

between the lower- and higher-Dust7–12 subsets. Effective ice particle radius decreased significantly, from 31.90 to 28.44 µm (r_{rb}=-0.36, q=0.0023), while OLR decreased from 215.0 to 192.6 W m^{-2} (r_{rb}=-0.44, q<0.001). During summer, the principal significant within-SDE difference was observed for high-cloud fraction (0.199 versus 0.497, r_{rb}=0.50, q<0.001), whereas autumn showed significant differences primarily in cloud-top pressure (405 versus 278 hPa, r_{rb}=-0.57, q=0.0022) and cloud-top temperature (238.1 versus 228.0 K, r_{rb}=-0.54, q=0.0035).

Long-term trends of dust and cirrus cloud relationships in spring

Based on the seasonal analysis above, the long-term assessment was focused on spring, which combined the largest number of identified SDEs and the highest mean dust loading with the most coherent dust-dependent responses across cirrus reflectance, high-cloud fraction, cloud-top properties, and OLR.

The five-year analysis revealed substantial temporal variability in springtime SDE-associated cloud properties without a corresponding monotonic increase in upper-tropospheric dust loading. Median Dust7–12 during spring SDEs varied between 6.73×10^{-8} and 1.29×10^{-7} kg kg^{-1}, with the lowest value occurring in 2016–2020 and no systematic increase towards the end of the record. In contrast, the cirrus reflectance anomaly during high-Dust7–12 SDEs increased markedly: relative to the corresponding low-dust background, median cirrus reflectance was 143% higher in 2001–2005, 147% in 2006–2010, 318% in 2011–2015, 327% in 2016–2020, and 398% in 2021–2025. The absolute median cirrus reflectance increased from 0.116 in 2001–2005 to 0.223 in 2021–2025, while the corresponding background values remained similar (0.048 and 0.045, respectively).

Other cloud properties showed persistent but less monotonic differences. High-cloud fraction during high-Dust7–12 SDEs was 122–161% above background during 2001–2015, 54% higher in 2016–2020, and 135% higher in 2021–2025. Cloud-top pressure remained 25–34% lower and cloud-top temperature approximately 5–7% lower than background throughout the five periods, with the largest recent differences occurring in 2021–2025. Effective ice particle radius showed greater temporal variability: the anomaly changed from +2.8% in 2001–2005 to −15.7% in 2006–2010, −8.3% in 2011–2015, approximately zero in 2016–2020, and −7.7% in 2021–2025. OLR remained lower during high-Dust7–12 SDEs in every period, with differences ranging from approximately −10% to −17%. Thus, among the investigated variables, the clearest five-year change was observed in cirrus reflectance, whose SDE-associated enhancement became substantially larger over the study period despite the absence of a parallel increase in Dust7–12.